A Flow Sensing Model for Mesenchymal Stromal Cells Using Morphogen Dynamics

Michael Gortchacow, Alexandre Terrier, and Dominique P. Pioletti*
Laboratory of Biomechanical Orthopedics, École Polytechnique Fédérale de Lausanne, Lausanne, Switzerland

ABSTRACT The differentiation of mesenchymal stromal cells has been shown to be affected by many parameters such as morphogens, flow rate, medium viscosity, and shear stress when exposed to fluid flow. The mechanism by which these cells sense their environment is still under intense discussion. In particular, during flow chamber experiments, it is difficult to interpret the interplay of the above-mentioned parameters in the process of cell differentiation. In this work, we tested the hypothesis that the competition between diffusion and advection of paracrine morphogens could explain the dependency of the cell differentiation to the above-mentioned parameters. To evaluate this hypothesis, we developed a numerical model simulating a simplified version of the advection-diffusion-reaction of morphogens secreted by the cells within a flow chamber. The model predicted a sharp transition in the fraction of receptors bound to the morphogen. This transition was characterized by a new, dimensionless number depending on flow rate, flow viscosity, flow chamber dimensions, and morphogen decay rate. We concluded that the competition between diffusion and advection of paracrine morphogens can act as a probe for the cells to sense their pericellular environment.

INTRODUCTION

Mesenchymal stromal cell (MSC) differentiation is central in normal organism development and maintenance, capable of differentiation into adipocytes, chondrocytes, and osteoblasts (1). The understanding of MSC differentiation mechanisms has implications in developmental biology, for pathophysiology aspects such as for cancer and osteointegration of implants.

Soluble growth factors have been clearly identified and demonstrated to be involved in MSC differentiation (1). These factors, such as members of the TGF-β superfamily, FGF, VEGF, and Wnt among others, are involved in the differentiation of MSC into osteoblastic lineage (2–6). Soluble growth factors have been originally proposed and termed "morphogens" by Turing (7). Morphogens are ligands that bind reversibly to transmembrane receptors and initiate signal transduction cascades that regulate the cell's differentiation pathway (8,9).

In addition to morphogens, recent experiments made with flow chambers demonstrated that mechanical stimulus generated by fluid flow plays a role in the differentiation process of plated MSCs (2,10–14). Direct mechanical loading of MSC through shear stress induced by fluid flow stimulate late osteogenic markers (14). The shear stress depends on the culture medium's flow rate, the viscosity, as well as the flow chamber's dimensions. Whether MSC's differentiation response to flow occurs as a result of chemotransport, direct mechanical stimuli, or both, remains largely unknown in flow chamber experiments. From the experimental results obtained in flow chambers, it can be concluded that MSCs have developed capabilities to sense their environment. To explain these sensitivity capabilities, we developed a numerical model simulating a simplified version of the advection-diffusion-reaction of morphogens secreted by the cells within a flow chamber. With this model, we tested the hypothesis that the competition between diffusion and advection processes of paracrine morphogens can act as a probe for the cells to sense their pericellular environment.

METHODS

Advection-diffusion-reaction model

In most flow chamber experiments with MSCs and osteoblasts where a response to flow is observed (2,10–14), the corresponding shear stress on the cells is ~1 Pa. The flow is of Poiseuille type with low Reynolds and Womersley numbers (15). In our study, we consider a steady-state flow as it was in the experimental conditions of Kreke et al. (14). The dimensionless advection-diffusion-reaction equation at constant temperature and low density of ligands is (16)

$$\frac{\partial}{\partial t}C = \left(\alpha^2\frac{\partial^2}{\partial x^2}C + \frac{\partial^2}{\partial y^2}C\right) - y(1-y)Pe\frac{\partial}{\partial x}C - \chi C, \quad (1)$$

where C is the dimensionless ligand concentration, α is the ratio of chamber height h to cell colony length L, Pe is the Péclet number, and χ is the ratio between the decay rate $(1/\tilde{\tau})$ and the diffusive rate D of the ligand. The definition of all dimensionless numbers is given in the Appendix.

The exact nature of the morphogen degradation is not currently known. Several possibilities could be considered to model this phenomenon such as multiple interacting morphogens and antagonists with or without receptor-mediated trafficking. As experimental data are not available in general

Submitted September 4, 2012, and accepted for publication April 8, 2013.

*Correspondence: dominique.pioletti@epfl.ch

Editor: Denis Wirtz.

0006-3495/13/05/2132/5 $2.00

http://dx.doi.org/10.1016/j.bpj.2013.04.014

for characterizing the morphogen degradation, we have chosen the simplest model possible. We assume an antagonist in excess, with a low binding rate to the morphogen, modeled as decaying the latter at a constant decay. With this approach, we limit the number of unknown variables to be introduced in the model. The kinetics of the ligand binding the receptor on the cell membrane follows the description proposed by Edwards (17),

$$\frac{\partial}{\partial t}B = k_{\text{on}}\Big[(1-B)C\big|_{y=0} - KB\Big], \tag{2}$$

where B is the ratio between the surface concentration of bound receptors to the total number of receptors R_T, k_{on} is the dimensionless reaction rate, and K is the dimensionless version of $\tilde{K}$ representing the binding affinity (ratio of the associate rate constant $\tilde{k}_{\text{on}}$ to the dissociation rate constant $\tilde{k}_{\text{off}}$). More details can be found in the Appendix.

We consider a paracrine production of ligands with a constant dimensionless secreted rate γ. This dimensionless secretion rate appears in the boundary condition at the cell surface, which is

$$\gamma - \frac{\partial}{\partial t}B = -D_D\frac{\partial}{\partial y}C\bigg|_{y=0}, \tag{3}$$

where D_D is a normalized diffusion coefficient (see Appendix for details). Equation 3 represents the flux out of the surface, which is equal to the difference between the secretion rate and the rate of change of the bound receptor concentration (16). The system in Eqs. 1–3 is characterized by seven parameters: χ, α, Pe, D_D, γ, k_{on}, and K. We will use

$$Da_\gamma = \frac{\gamma}{D_D} \text{ and } Da = \frac{k_{\text{on}}}{D_D}.$$

instead of γ and k_{on}. Da_γ and Da are the Damköhler numbers representing the ratios between rate of production of ligands to diffusive rate and reaction rate to diffusive rate, respectively.

To analyze the effect of flow and other parameters on the number of cell bound receptors, we defined $B_s^{Pe=0}$ with the value of B corresponding to the stationary solution in static culture conditions, or reference state. Given the parameters of the model, the reference state approximates well to an infinite epithelia of MSC with no flow ($Pe = 0$). We use $B/B_s^{Pe=0}$ to measure the variation in the number of receptors. We expect a cellular response when the number of bound receptors changes significantly, i.e., $B/B_s^{Pe=0} \gg 1$.

Parameters used in the model

For h, L, and the maximal flow velocity in the chamber, we use the values from the experimental setup of Kreke et al. (14) (see Table 1). We consider TGF-β, FGF, VEGF, and Wnt as possible candidates for the ligand of our model. Their molecular masses range approximately between 25 and 60 kDa. Using the Einstein-Stokes equation to estimate the diffusivity of the ligand and a protein density of 1.43 g/cm^3 (18), we find that $D \simeq 100\ \mu\text{m}^2/\text{s}$.

The value for the binding affinity appearing in Eq. 2 is obtained from published experimental data (19,20).

TABLE 1 Parameters from literature

Parameter	Value/range	Source	Description
D	100 μm^2/s	See text	Diffusivity
L	60 mm	(14)	Epithelia length
h	250 μm	(14)	Chamber height
$\tilde{K}$	20 nM	(19)	Binding affinity
$\tilde{k}_{\text{on}}$	3×10^4 M^{-1} s^{-1}	(19)	Association constant
R_T	10^{-8} pmol/μm^2	(20)	Receptor's surface density
$1/\tilde{\tau}$	1.6–1.6 $\times$ 10^{-5} s^{-1}	(21,22)	Decay rate

The decay rate of the morphogens is not known; however, they have been estimated to range from 10^{-4} s^{-1} (21) to 0.2 s^{-1} (22). We solve the model for a set of $1/\tilde{\tau}$ ranging between 1.6×10^{-5} s^{-1} and 1.6 s^{-1}. This range of $1/\tilde{\tau}$, together with the values of D and h, translate into $10^{-2} < \chi < 10^3$.

For the rest of the undetermined dimensionless parameters, the values are chosen to be as close to unity as possible, so as to have all terms of Eqs. 2 and 3 influencing the solution. An additional constraint was added to have the receptors of the reference state ranging from unsaturated ($B_s^{Pe=0} \sim 0$) to saturated ($B_s^{Pe=0} \sim 1$). As a result, the maximum concentration of the ligand of the reference state ranged from 20 pM to 60 nM.

With D, h, L, and the maximal flow velocity defined, we obtain $Pe = 467$ for the above-mentioned experiment. Therefore, as we want to study the effect the flow has on bound receptors, we vary Pe from 0 to 1000. All dimensionless parameters used are shown in Table 2. The initial and boundary conditions of the ligand concentration are reported in the Appendix.

RESULTS AND DISCUSSION

The reference state

The reference state $B_s^{Pe=0}$ reduces to (see Appendix for details)

$$B_s^{Pe=0} = \frac{C_s^{Pe=0}\big|_{y=0}}{C_s^{Pe=0}\big|_{y=0} + K} = \frac{\frac{1}{\sqrt{\chi}}\text{Coth}\left[\sqrt{\chi}\right]}{\frac{1}{\sqrt{\chi}}\text{Coth}\left[\sqrt{\chi}\right] + \frac{K}{Da_\gamma}}, \tag{4}$$

which shows that when

$$\frac{K}{Da_\gamma} \ll \frac{1}{\sqrt{\chi}}\text{Coth}\left[\sqrt{\chi}\right],$$

the receptors saturate ($B_s^{Pe=0} = 1$) and for

$$\frac{K}{Da_\gamma} \gg \frac{1}{\sqrt{\chi}}\text{Coth}\left[\sqrt{\chi}\right],$$

most receptors remain unbound. As described in the Appendix, the characteristic distance of penetration of the ligand along the height of the chamber is approximately equal to 1 for $\chi < 1$ and $\chi^{-1/2}$ for $\chi > 1$. We name this distance, the penetration distance of the morphogen.

When do cells sense the flow?

As soon as the flow is applied, in particular with $Pe >> 1$, the center of the flow chamber becomes advective-dominant. However, within the vicinity of the cells, the advective term is negligible and the solution will be diffusive-dominant (*inset* in Fig. 1). The limit between these two regions is called the diffusive boundary layer.

TABLE 2 Dimensionless parameters of the model

Dimensionless parameter	Value/range	Source
Da_γ	3.15	See text
Da	0.75	See text
Pe	0–10^3	Estimated (14,22)
χ	10^{-2}–10^3	Derived from h, D, and $\tilde{\tau}$
D_D	0.5	See text
K	100	See text
α	4.1×10^{-3}	(14)

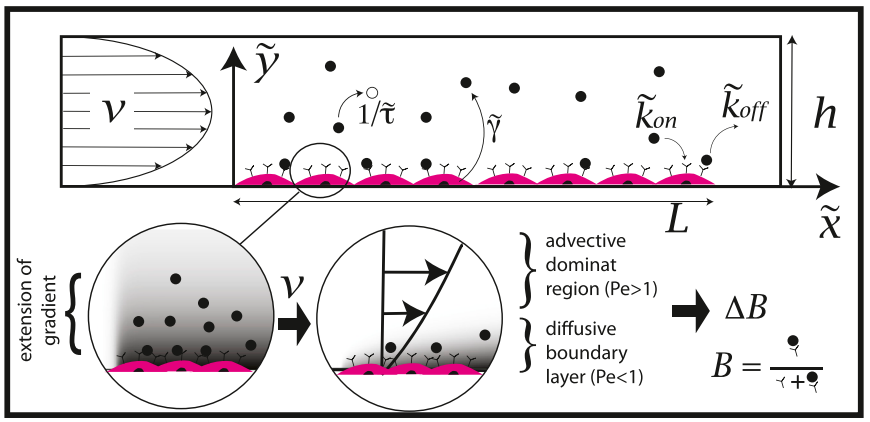

FIGURE 1 Illustration of the model. A morphogen is secreted by the cells, has a decay rate in the bulk, and reacts reversibly with receptors on the cells. This will generate a gradient of morphogens within the medium (*bottom-left inset*). Varying the cellular environment described by parameters of the model such as the chamber geometry, the flow (*bottom-right inset*), the decay rate of the morphogen, etc., will induce a change in the gradient. A gradient change in turn will change B (ratio between the number of bound receptors and the total number of receptors), indicating to what extent the cells will sense the change in the pericellular environment.

If the flow disrupts the ligand concentration, a change in the number of bound receptors is expected. However, when the diffusive boundary layer engulfs the ligands, the solution is mainly diffusive-dominant and similar to the reference state, with no expected cellular response. Both the disrupted and nondisrupted ligand concentrations were solved numerically (Fig. 2). Details on the numerical aspects can be found in the Appendix.

To determine the boundary layer thickness, we substitute the ligand concentration (C) and the fraction of bound ligands on the cell surface (B) in all equations of the model by their Taylor series, with Pe^{-1} as a perturbation parameter, and retain the first order. By doing so, and considering the values used, it can be shown (see Edwards (17) for methodology) that the diffusive boundary layer has a thickness that goes as $Pe^{-1/3}$ as well as being dependent on x (Fig. 2).

Having quantified the boundary layer thickness, the ratio between the penetration distance of the morphogen and the boundary layer goes as $Pe^{1/3}\chi^{-1/2}$, for $\chi > 1$. The dependency of $\overline{B}_s/B_s^{Pe=0}$ on $Pe^{1/3}\chi^{-1/2}$ for the case considered is shown in Fig. 3. $\overline{B}$ is the average of B and reflects the experimental results where most techniques (such as qPCR, immunofluorescence, cell staining, Western blots, measure $[Ca^{++}]$, etc.) average-out the cell response. We clearly observe a transition near 1, which occurs when the penetration distance of the morphogen equals to the boundary layer thickness (Fig. 3). For the case studied, the cells are responsive to flow when

$$Pe^{\frac{1}{3}}\chi^{-\frac{1}{2}} \gtrsim 1. \tag{5}$$

Therefore, the transition between cell sensing and cell not sensing the flow could be characterized by the new dimensionless number $Pe^{1/3}\chi^{1/2}$.

In its dimensional form, Eq. 5 becomes

$$f(L)\frac{V^2}{\mu L^2 h^2}\tilde{\tau}^3 \gtrsim C_m, \tag{6}$$

with C_m being a constant proportional to the hydrodynamic radius of the morphogen and inversely proportional to the temperature (considered constant). The value $f(L)$ is some function of L, as the boundary layer increases with x. We may appreciate from Eq. 6 that there is a stronger dependency of the cellular response on V than on μ. This stronger

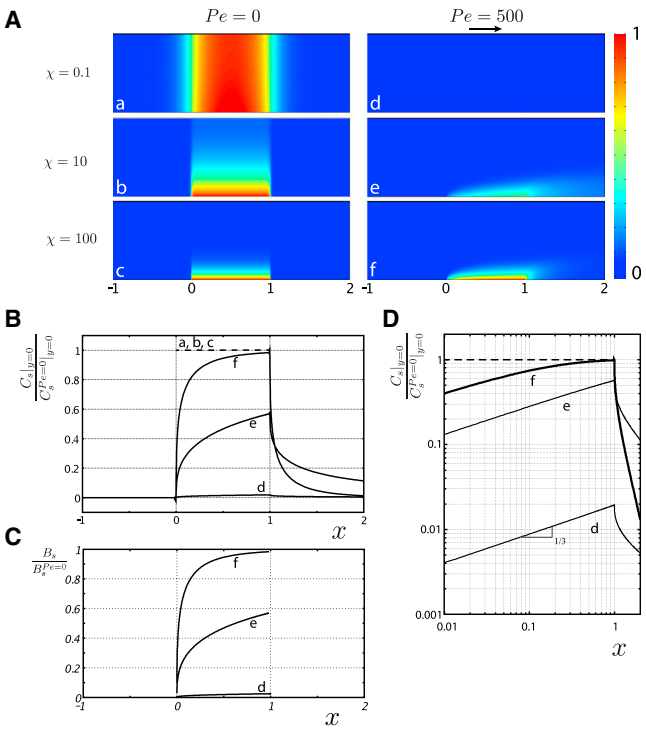

FIGURE 2 (*A*) Surface plot of the normalized ligand concentration along the fluidic channel, $C_s^{Pe}/C_s^{Pe=0}(y=0)$. The reference state without flow (*a–c*) and the corresponding cases with flow ($Pe = 500$) (*d–f*, respectively), for three different dimensionless decay rates $\chi = 10^{-1}$, 10^1, and 10^2. (*B*) The normalized ligand concentration at the cell surface for the corresponding χ values when flow is applied. (*C*) The resulting fold change of the number of bound ligands ($B_s^{Pe=500}/B_s^{Pe=0}$). When the ligand penetration into the chamber (determined by χ) is relatively smaller than the boundary layer thickness (determined by Pe), the cells are not expected to react differently when flow is applied (case *f*). However, when the converse is true (cases *e* and *d*), the fraction of bound ligands changes substantially, resulting in a response to flow. (*D*) Log-log plot of B, showing clearly how cells upstream are more affected by flow than cells downstream.

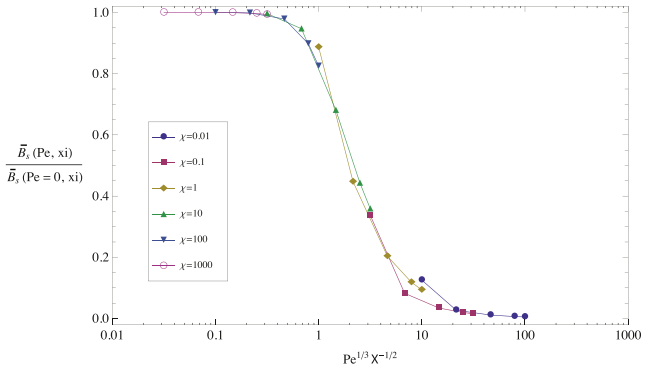

FIGURE 3 Fold change of the mean value of bound receptors on the cell surface, $\overline{B}_s(Pe)/B_s^{Pe=0}$, as a function of $Pe^{1/3}\chi^{-1/2}$. For the parameters used, $Pe^{1/3}\chi^{-1/2}$ is the ratio between the characteristic distance of the ligand concentration profile, which is $\chi^{-1/2}$ and the boundary layer (and has a thickness of $Pe^{-1/3}$, see text). A clear transition appears when the boundary layer and the ligand profile distances are similar. Initial condition of B is considered from the reference state with no flow.

dependency has been observed experimentally (12,23). It is interesting to note that the shear stress is a function of h, V, and μ. The dependency of differentiation on shear stress may then be a result of h, V, and μ appearing in Eq. 6.

As previously mentioned, the diffusive boundary layer is not constant along the flow stream (x coordinate). In similar reactive diffusive equations, this layer goes as $Pe^{1/3}\chi^{1/3}$ (except in the boundaries; see Edwards (17)). It means that the boundary layer gets thicker downstream, inducing then a gradient on the bound ligands along the flow stream. Upstream, where the boundary layer is smaller, the advective effects are stronger, therefore inducing a greater change of $B_s/B_s^{Pe=0}$ with respect to downstream cells (Fig. 2 *c*).

CONCLUSION

The plethora of interactions among the morphogens, antagonists, receptors, and proteins governing the MSC differentiation are highly complex and largely unknown. In the context of a flow chamber experiment, we developed a simplified model involving a paracrine morphogen with a constant decay rate allowing us to replicate experimental observations of MSC sensing flow. The model predicts cell response to the flow rate and the viscosity of the media, as observed experimentally.

Many parameters can vary between flow chamber experiments. Direct comparison of the results is then difficult. With the developed model, a dimensionless number was defined, allowing us to determine the transition between cells sensing and not sensing the flow. This dimensionless number might then facilitate comparisons between experiments. The biological interpretation of flow chamber experiments, with respect to differentiation, for example, could be done without taking into account the dimensions or flow characteristics of the flow chamber.

The model also predicts a different response between cells up- and downstream of the flow chamber, a result yet to be observed experimentally.

APPENDIX

Advection-diffusion-reaction model

The directions along and perpendicular to the cell surface are $\tilde{x}$ and $\tilde{y}$, respectively. The value $\tilde{t}$ is the time, h is the height of the flow chamber, and $v(\tilde{y},\tilde{t})$ is the velocity along the $\hat{x}$ direction (Fig. 1). We define the dimensionless parameters

$$x = \frac{\tilde{x}}{L},\ y = \frac{\tilde{y}}{h},\ t = \frac{D}{h^2}\tilde{t},\ \chi = \frac{h^2}{D}\frac{1}{\tilde{\tau}},$$
$$\alpha = \frac{h}{L},\ C = \frac{\tilde{C}}{C_T},\ Pe = \frac{h^2 V}{LD},$$

where L is the length of the cell colony, D is the diffusivity of the ligand, χ is the ratio between the decay rate $(1/\tilde{\tau})$ and the diffusive rate of the ligand, $\tilde{C}$ is the ligand concentration, C_T is a concentration used for scaling $\tilde{C}$, V is four times the maximum flow velocity in the chamber, and Pe is the Péclet number.

With these definitions, the dimensionless advection-diffusion-reaction equation for constant temperature and low density of ligands is given by Eq. 1. We name $\tilde{k}_{on}$ and $\tilde{k}_{off}$ the association and dissociation constants, respectively, for the ligands with the receptors. The binding affinity is $\tilde{K} = \tilde{k}_{off}/\tilde{k}_{on}$. We define the surface concentration of total number of receptors as R_T. Although R_T is not constant in time as it depends on the cell's metabolism, we will consider its variation negligible during the time of the experiment. We define B as the ratio between the surface concentration of bound receptors and R_T, $k_{on} = \tilde{k}_{on}C_T h^2/D$, and $K = \tilde{K}/C_T$. Using the same nomenclature as in Edwards (17), Eq. 2 on the reactive surface is obtained.

Initial and boundary conditions

As the ligands concentration is proposed to play a central role in the sensory capabilities of the MSC, we need to clearly define the initial and boundary conditions for this variable. In this study, we consider a paracrine production of ligands with a constant secreted rate $\tilde{\gamma}$. Its dimensionless value is $\gamma = \tilde{\gamma}h^2/DR_T$. This dimensionless secretion rate appears in the boundary condition at the cell surface in Eq. 3. In this equation, $D_D = C_T h/R_T$. The boundary conditions at the chamber entrance, at the downstream end, and at the channel ceiling, are given (24), respectively, by

$$C|_{x=-\infty} = 0,\ \frac{\partial}{\partial x}C\bigg|_{x=\infty} = 0 \text{ and } \frac{\partial}{\partial y}C\bigg|_{y=1} = 0. \quad (7)$$

Finally, the boundary condition outside the chamber is given by

$$\frac{\partial}{\partial y}C\bigg|_{y=0} = 0,\ \text{for } x<0 \text{ and } 1<x. \quad (8)$$

The reference state

To obtain the reference state $B_s^{Pe=0}$, it is necessary to obtain the stationary solution for the ligand concentration, $C_s^{Pe=0}$. The solution reduces to solving Eqs. 1, 3, and 7 with $C = C_s^{Pe=0}(y)$ and is given by

$$C_s^{Pe=0}(y) = \frac{Da_\gamma}{\sqrt{\chi}}\mathrm{Cosh}\left[\sqrt{\chi}(1-y)\right]\mathrm{Csch}\left[\sqrt{\chi}\right]. \quad (9)$$

At the cell boundary, $C_s^{Pe=0}$ becomes

$$C_s^{Pe=0}\big|_{y=0} = \frac{Da_\gamma}{\sqrt{\chi}}\mathrm{Coth}\left[\sqrt{\chi}\right]. \tag{10}$$

From Eq. 9, $C_s^{Pe=0}(y)$ depends linearly on Da_γ. Therefore, the decay profile of ligand concentration along the height of the channel depends solely on χ with a maximum concentration of $C_s^{Pe=0}(0)$ at the cell surface. Using Eqs. 9 and 10, we normalize $C_s^{Pe=0}(y)$ so as to have a maximum value of 1. The normalized profile is

$$\frac{C_s^{Pe=0}(y)}{C_s^{Pe=0}(0)} = \mathrm{Cosh}\left[(-1+y)\sqrt{\chi}\right]\mathrm{Sech}\left[\sqrt{\chi}\right] \simeq \begin{cases} e^{-\sqrt{\chi}y} & \text{for } \chi>1 \\ 1 & \text{for } \chi<1 \end{cases}. \tag{11}$$

From Eq. 11, we obtain a characteristic distance for the profile of the ligand along the height of the chamber. This characteristic distance is approximately equal to 1 for $\chi < 1$ and $\chi^{-1/2}$ for $\chi > 1$. In its dimensional form, the characteristic distances are h for $\chi < 1$ and $h/\sqrt{\chi} = \sqrt{D\tilde{\tau}}$ for $\chi > 1$. As the normalized profile is independent of h for $h \to \infty$, it means that χ determines whether or not the chamber height is within the reach of the morphogen profile. Using Eqs. 2 and 10, we obtain the fraction of bound morphogens for the reference state given by Eq. 4.

Numerical approximations

For the reference state, the model is solved analytically (see Eq. 4). However, to study the effect of flow, the model is solved numerically. For the first two boundary conditions from Eq. 7, we replace $-\infty$ and ∞ by -1 and 2, respectively. This approximation proves satisfactory for all simulations performed. It results in a rectangular domain with x coordinates spanning from -1 to 2 and y from 0 to 1. The reactive cell surface is placed at $y = 0$ between $x = 0$ and $x = 1$. The mesh consists of 8400 rectangular elements, with a higher density near the reactive surface. The code is validated with the analytically found stationary solution. The solutions are computed using COMSOL 3.5a (Comsol, Palo Alto, CA).

This study was funded by the Swiss National Science Foundation (No. 320030-125498), and the Inter-Institutional Center for Translational Biomechanics, École Polytechnique Fédérale de Lausanne-Centre Hospitalier Universitaire Vaudois-Le Département de l'Appareil Locomoteur.

REFERENCES

1. Pittenger, M. F., A. M. MacKay, …, D. R. Marshak. 1999. Multilineage potential of adult human mesenchymal stem cells. *Science.* 284: 143–147.
2. Arnsdorf, E., P. Tummala, and C. Jacobs. 2009. Non-canonical Wnt signaling and N-cadherin related b-catenin signaling play a role in mechanically induced osteogenic cell fate. *PLoS ONE.* 4:e5388.
3. Gregory, C. A., D. J. Prockop, and J. L. Spees. 2005. Non-hematopoietic bone marrow stem cells: molecular control of expansion and differentiation. *Exp. Cell Res.* 306:330–335.
4. Dimitriou, R., E. Tsiridis, and P. V. Giannoudis. 2005. Current concepts of molecular aspects of bone healing. *Injury.* 36:1392–1404.
5. Stappenbeck, T. S., and H. Miyoshi. 2009. The role of stromal stem cells in tissue regeneration and wound repair. *Science.* 324:1666–1669.
6. Krishnan, V., H. U. Bryant, and O. A. MacDougald. 2006. Regulation of bone mass by Wnt signaling. *J. Clin. Invest.* 116:1202–1209.
7. Turing, A. M. 1952. The chemical basis of morphogenesis. *Philosoph. Trans. Roy. Soc. Lond. B Biol. Sci.* 237:37–72.
8. Christian, J. L. 2000. BMP, Wnt and Hedgehog signals: how far can they go? *Curr. Opin. Cell Biol.* 12:244–249.
9. Ashe, H. L., and J. Briscoe. 2006. The interpretation of morphogen gradients. *Development.* 133:385–394.
10. Glossop, J. R., and S. H. Cartmell. 2009. Effect of fluid flow-induced shear stress on human mesenchymal stem cells: differential gene expression of IL1B and MAP3K8 in MAPK signaling. *Gene Expr. Patterns.* 9:381–388.
11. Li, Y. J., N. N. Batra, …, C. R. Jacobs. 2004. Oscillatory fluid flow affects human marrow stromal cell proliferation and differentiation. *J. Orthop. Res.* 22:1283–1289.
12. Riddle, R. C., K. R. Hippe, and H. J. Donahue. 2008. Chemotransport contributes to the effect of oscillatory fluid flow on human bone marrow stromal cell proliferation. *J. Orthop. Res.* 26:918–924.
13. Riddle, R. C., A. F. Taylor, and H. J. Donahue. 2008. Fluid flow assays. *Methods Mol. Biol.* 455:335–345.
14. Kreke, M. R., W. R. Huckle, and A. S. Goldstein. 2005. Fluid flow stimulates expression of osteopontin and bone sialoprotein by bone marrow stromal cells in a temporally dependent manner. *Bone.* 36:1047–1055.
15. Leal, L. 1992. Laminar Flow and Convective Transport Processes. Butterworth-Heinemann Series in Chemical Engineering. Butterworth-Heinemann, Boston.
16. Welty, J. R. 2001. Fundamentals of Momentum, Heat, and Mass Transfer. Wiley, New York.
17. Edwards, D. 1999. Estimating rate constants in a convection-diffusion system with a boundary reaction. *IMA J. Appl. Math.* 63:89–112.
18. Quillin, M. L., and B. W. Matthews. 2000. Accurate calculation of the density of proteins. *Acta Crystallogr. D Biol. Crystallogr.* 56: 791–794.
19. Bourhis, E., C. Tam, …, R. N. Hannoush. 2010. Reconstitution of a Frizzled-8.Wnt3a.LRP6 signaling complex reveals multiple Wnt and Dkk1 binding sites on LRP6. *J. Biol. Chem.* 285:9172–9179.
20. MacGabhann, F., J. W. Ji, and A. S. Popel. 2006. Computational model of vascular endothelial growth factor spatial distribution in muscle and pro-angiogenic cell therapy. *PLOS Comput. Biol.* 2:e127.
21. Bailón-Plaza, A., and M. C. van der Meulen. 2001. A mathematical framework to study the effects of growth factor influences on fracture healing. *J. Theor. Biol.* 212:191–209.
22. Fleury, M. E., K. C. Boardman, and M. A. Swartz. 2006. Autologous morphogen gradients by subtle interstitial flow and matrix interactions. *Biophys. J.* 91:113–121.
23. Donahue, T. L. H., T. R. Haut, …, C. R. Jacobs. 2003. Mechanosensitivity of bone cells to oscillating fluid flow induced shear stress may be modulated by chemotransport. *J. Biomech.* 36:1363–1371.
24. Edwards, D. A., B. Goldstein, and D. S. Cohen. 1999. Transport effects on surface-volume biological reactions. *J. Math. Biol.* 39:533–561.